ACS APPLIED MATERIALS & INTERFACES

LETTER

www.acsami.org

Nanoporous Thermochromic VO_2 Films with Low Optical Constants, Enhanced Luminous Transmittance and Thermochromic Properties

Litao Kang,[†,‡] Yanfeng Gao,[*,†] Hongjie Luo,[*,†] Zhang Chen,[†] Jin Du,[†] and Zongtao Zhang[†]

[†]State Key Laboratory of High Performance Ceramics and Superfine Microstructure, Shanghai Institute of Ceramics (SIC), Chinese Academy of Sciences (CAS), Dingxi 1295, Changning, Shanghai, 200050, China

[‡]Graduate University of Chinese Academy of Sciences, Yuquanlu 19, Beijing, 100049, China

ABSTRACT: Nanoporous thermochromic VO_2 films with low optical constants and tunable thicknesses have been prepared by polymer-assisted deposition. The film porosity and thickness change the interference relationship of light reflected from the film−substrate and the air−film interfaces, strongly influencing the optical properties of these VO_2 films. Our optimized single-layered VO_2 films exhibit high integrated luminous transmittance ($T_{lum,l}$ = 43.3%, $T_{lum,h}$ = 39.9%) and solar modulation (ΔT_{sol} = 14.1%, from $T_{sol,l}$ = 42.9% to $T_{sol,h}$ = 28.8%), which are comparable to those of five-layered $TiO_2/VO_2/TiO_2/VO_2/TiO_2$ films ($T_{lum,l}$ = 45%, $T_{lum,h}$ = 42% and ΔT_{sol} = 12%, from $T_{sol,l}$ = 52% to $T_{sol,h}$ = 40%, from *Phys. Status Solidi A* **2009**, *206*, 2155−2160.). Optical calculations suggest that the performance could be further improved by increasing the porosity.

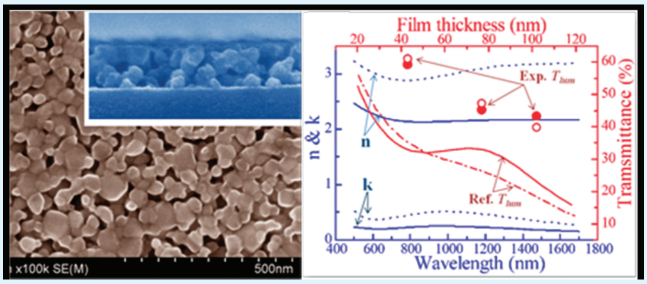

KEYWORDS: vanadium dioxide, optical property, thermochromic property, porosity

Fully reversible metal−insulator transitions (MIT) could be triggered in the monoclinic/rutile (M/R)-phase VO_2 by temperature,[1] strain,[2] electric field,[3] or optical excitation.[4] This transition is distinguished by a dramatic change of optical/electric properties,[1,5] a fast switching time,[4] and a tunable switching temperature,[2] and may thus have applications that include resistive switching elements, optical storage devices, light modulators, and smart windows.[6]

For the practical application of VO_2-based smart windows, a low luminous transmittance (T_{lum}) and solar modulating ability (ΔT_{sol}) are two major drawbacks.[7] The T_{lum} and T_{sol} values were obtained from $T_{lum,sol}(\tau) = \int \varphi_{lum,sol}(\lambda)T(\lambda,\tau)d\lambda / \int \varphi_{lum,sol}(\lambda)d\lambda$, where φ_{lum} is the spectral sensitivity of the light-adapted eye and φ_{sol} is the solar irradiance spectrum for an air mass of 1.5 (corresponding to the sun standing 37° above the horizon). ΔT_{sol} is obtained from $\Delta T_{sol} = T_{sol,l} - T_{sol,h}$, where l and h denote low- and high-temperature, respectively.

Strategies to improve T_{lum} and ΔT_{sol} have been investigated, including Mg- or F-doping,[8,9] multilayer-stack design,[10,11] and composite film construction.[12] Besides a depression in transition temperature, Mg- or F-doping causes a blueshift in the absorption edge of VO_2 films (from around 445 to 415 nm[8]). This change results in a significant increase of the luminous transmittance at the expense of infrared modulating ability (wavelength ≥ 1000 nm).[9] Similar trade-offs between the luminous transmittance and thermochromic properties have also been observed in VO_2-based multilayer films.[11] A VO_2−SiO_2 composite film shows a high visible transmittance but weak infrared modulating ability.[12] Five-layered $TiO_2/VO_2/TiO_2/VO_2/TiO_2$ films with optically optimized structures have a relatively higher luminous transmittance and solar modulating ability.[7] However, incorporating dielectric layers with a certain refractive index and thickness into complicated stack structures is a difficult technological challenge. Optical calculations suggest that VO_2 nanoparticles distributed in a dielectric matrix have higher T_{lum} and ΔT_{sol} than pure VO_2 films.[13a] This study further predicts that a limit for noticeable solar energy modulation is T_{lum} = 40%, and $\Delta T_{sol} \leq$ 10%.[13a] We have recently confirmed experimentally the effects of composite matrix.[13b] VO_2−ZrV_2O_7 composite films with similar thickness of about 95 nm showed decreased particle sizes and significantly enhanced luminous transmittances (from 32.3% at Zr/V = 0 to 53.4% at Zr/V = 0.12) with increasing Zr/V rations.

However, the influence of porosity on optical properties of single-layered VO_2 films, which should have priority over the stack structure of VO_2-based multilayers, is seldom reported. Pores with air in VO_2 films can be considered as a secondary component that should have similar effects on improving T_{lum} and ΔT_{sol}. After finishing this article, we paid attention to a Japanese open patent, JP2007−171759A, which mentioned that the increase in porosity favors the optical performance of VO_2 films mainly based on optical calculations.[14] In this paper, optical calculations confirm that optical constants and film thickness

Received: November 15, 2010
Accepted: January 17, 2011
Published: January 26, 2011

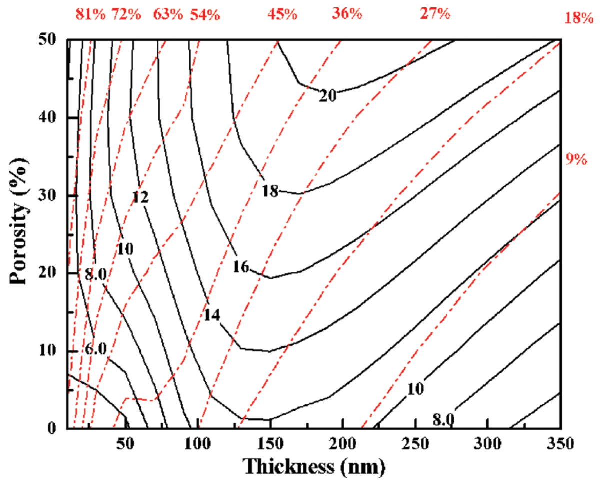

Figure 1. Computed luminous transmittance in an insulator state ($T_{lum,i}$, red dotted lines) and solar modulation between MIT (ΔT_{sol}, black solid lines) as a function of the thickness and porosity of the VO_2 films.

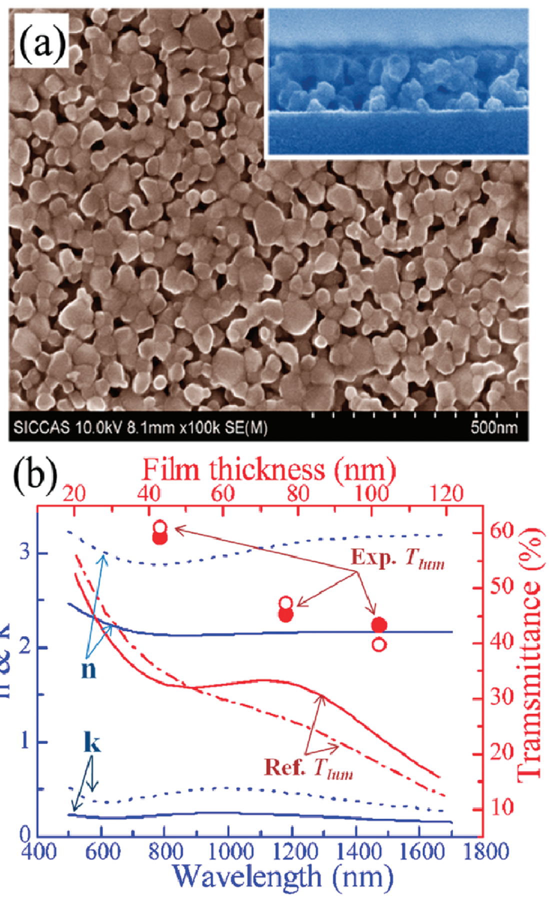

Figure 2. (a) SEM image of a 147 nm thick VO_2 films on quartz glass. The inset of part a is a cross-sectional SEM image. (b) Experimental (solid lines) and reference (dotted lines) optical constants at 20 °C as well as experimental (Exp. T_{lum}) and reference (Ref. T_{lum}) integral luminous transmittance of the film at 20 (solid symbols) and 90 °C (open symbols), respectively. The reference data are redrawn from ref 17.

have important effects on the thermochromic properties of these films. Furthermore, nanoporous VO_2 films with low optical constants

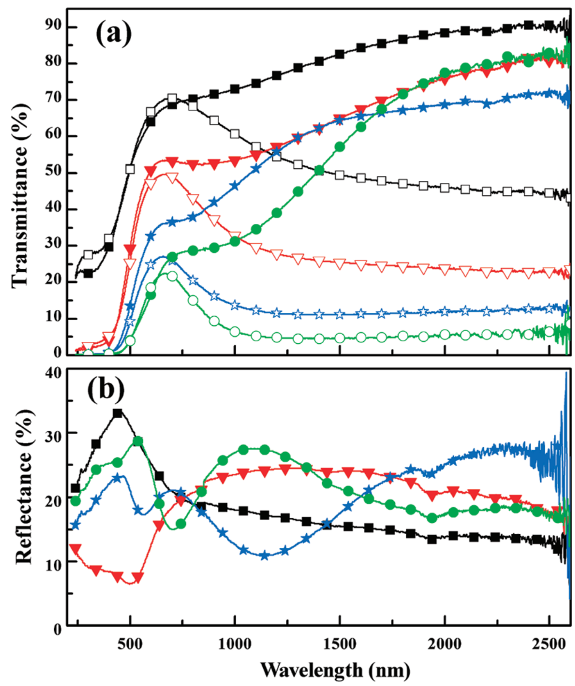

Figure 3. Thickness dependence of (a) transmittance and (b) reflectance spectra for typical samples with different thicknesses (43, 102, 215, and 428 nm corresponding to the black squares, the red triangles, the blue pentagrams and the green circles, respectively). The transmittance was measured at both 20 °C (lines with solid symbols) and 90 °C (lines with open symbols) and the reflectance was measured at only 20 °C.

and controllable thicknesses were prepared and showed enhanced optical properties as expected.

A 0.1 mol L^{-1} $VOCl_2$ aqueous solution containing polyvinylpyrrolidone (PVP, 6 wt %, K90) was spin-coated on fused silica substrates. After drying at 60 °C for 10 min, the resultant precursor films were annealed at 500 °C for 1 h with heating rate of 30 °C min^{-1} in a nitrogen atmosphere. The film thicknesses could be controlled by simply varying the spin-coating parameters. The optical properties and morphology of the films were then studied. The spectral transmittance and reflectance were measured using a Hitachi U-4100 double beam spectrophotometer. The transmission measurements were carried out at different temperatures using an in-house-developed heater module. A W-VASE with AutoRetarderTM ellipsometer was used to measure ellipsometric parameters of the films. The incident angles were 55 and 60°. The morphology was investigated by a JSM-6700F field-emission scanning electron microscope (FESEM).

An optical-admittance recursive method was used to simulate the spectral transmittance using the optical constants of VO_2 and a fused-silica-glass substrate. The optical constant is assumed to be linearly dependent on the volume fraction.[15,16] Figure 1 shows the computed luminous transmittance and solar modulation of VO_2 films with different thicknesses and porosities. The results indicate that ΔT_{sol} could be increased without decreasing T_{lum} by increasing the porosity, which is derived from the depression of the reflection.

To validate the above prediction, we prepared VO_2 films by a polymer-assisted deposition (PAD) method. X-ray diffraction and Raman spectra confirmed the formation of a monoclinic (M) phase with a trace amount of V_2O_5. Figure 2a shows a top-down SEM image of VO_2 films, which reveals that the sample consisted

Table 1. Optical Properties of Typical Samples with Different Thicknesses[a]

sample	thickness (nm)	$T_{sol,l}$ (%)	$T_{sol,h}$ (%)	ΔT_{sol} (%)	$T_{lum,l}$ (%)	$T_{lum,h}$ (%)	ΔT_{lum} (%)
I	43	62.1	55.7	6.4	59.2	61.1	−1.9
II	77	48.1	41.1	7.0	45.3	47.2	−1.9
III	102	42.9	28.8	14.1	43.3	39.9	3.4
IV	147	39.4	22.8	16.6	33.7	29.4	4.3
V	215	32.9	14.3	18.6	28.7	19.2	9.5
VI	428	23.0	9.2	13.8	11.5	12.6	−1.1

[a] *l* and *h* mean low-temperature (20 °C) and high-temperature (90 °C), respectively.

of interconnected VO_2 particles and irregular nanopores. The size of particle and pore ranges from 20 to 70 and 15 to 80 nm with a mean value of 38 and 28 nm, respectively. The feature size of the film is well below the wavelength of visible and infrared light, favoring the improvement of optical quality. The nanoporous feature of the films is observable for the entire film (inset of Figure 2a), which is also supported by the low n and k values of ellipsometry results compared with those in the literature (Figure 2b).[17] For example, the value of n is 2.2 for our VO_2 film, which is around 3 in the literature.[17] The result also shows that T_{lum} in the current research is much higher (by ≥ 12%) than that in the literature with comparable ΔT_{sol} because of the different optical constants (Figure 2b).[14,17] These results are attributed to the degradation of PVP and the shrinkage of the gel film during annealing.[5]

Figure 3 shows the transmittance and reflectance spectra of typical VO_2 films. The MIT transition is clearly observed as a dramatic infrared-transmittance change with temperature (Figure 3a). T_{lum} reduces steadily with increasing film thickness, which is ascribed to the strong absorption of VO_2 in this region.[13a,18] The change in the infrared transmittance of VO_2 films at 90 °C with different film thicknesses shows a similar behavior. Nevertheless, the infrared transmittance at 20 °C for a 428 nm thick film is obviously higher than that of a 215 nm thick film after 1700 nm (Figure 3a). These changes in the transmittance spectra correspond to reflectance valleys in Figure 3b, suggesting the existence of a self-antireflection effect in these thicknesses due to the destructive interference of light reflected from the film−substrate and the air−film interfaces.

The change in the optical constants of VO_2 across the MIT can effectively modulate the infrared transmittance and shift the position of the reflectance valley at 20 °C, leading to a significant enhancement of the IR modulating ability at a certain wavelength. This phenomenon could be harnessed to boost the thermochromic properties of a single-layer film in selected wavelength ranges. For instance, a 215 nm thick film shows a transmittance change of 50% (from 61.1 to 11.1%) at 1350 nm across the MIT, the highest value at this wavelength to our knowledge. Furthermore, the enhancement of the IR modulating ability could be adjusted to longer wavelengths by a simple regulation of the film thickness. A 428 nm thick VO_2 film exhibits a IR transmittance change of 76.5% (from 83 to 6.5%) at 2500 nm, even prior to the optimized result of sputtering films (74%).[19]

Another interesting phenomenon is that the changes in luminous transmittance (ΔT_{lum}) across the MIT are thickness dependent. For thin films, the visible transmittance at 20 °C is generally lower than that at 90 °C (Figure 3 and Table 1) and, vice versa. The visible transmittance at 20 °C for the above 100 nm thick films exceeds that at 90 °C (Figure 3b and Table 1). This reversion in ΔT_{lum} is ascribed to interference effects and was also reported by Xu et al.[17]

In view of the fact that solar energy is mainly in the visible region with a peak at 550 nm, the ΔT_{lum} reversion across the MIT effectively influences ΔT_{sol}. For instance, ΔT_{sol} increased by only 0.6% (from 6.4 to 7.0%) as the film thickness increased from 43 to 77 nm. Nevertheless, compared with the 77 nm thick film, ΔT_{sol} largely increased from 7.0 to 14.1% for the 102 nm thick film. Meanwhile, the $T_{lum,l}$ remained almost unchangeable (45.3 and 43.3% for the 77 and 102 nm thick films, respectively). Further increasing the film thickness to 147 and 215 nm increased ΔT_{sol} gently to 16.6 and 18.6%, accompanied by an evident depression in T_{lum}. Both T_{lum} and ΔT_{sol} were reduced for the 428 nm thick film. Therefore, the optimized thickness for films prepared by this system to balance T_{lum} and ΔT_{sol} is 100 nm. The single-layer film of this thickness shows comparable T_{lum} and ΔT_{sol} values to those of five-layered $TiO_2/VO_2/TiO_2/VO_2/TiO_2$ films with optically optimized structures ($T_{lum,l}$ = 45%, $T_{lum,h}$ = 42% and ΔT_{sol} = 12%, from $T_{sol,l}$ = 52% to $T_{sol,h}$ = 40%).[7]

In summary, we performed optical calculations for VO_2 films with different thicknesses and porosities. The results indicate that enhanced performance is expected with increased porosity and decreased optical constants. Consequently, we prepared VO_2 films with different thicknesses and with low optical constants via a PAD method. By cleverly controlling the film thicknesses, films with $T_{lum,l}$ = 43.3%, $T_{lum,h}$ = 39.9%, ΔT_{sol} = 14.1% (from $T_{sol,l}$ = 42.9% to $T_{sol,h}$ = 28.8%), ΔT = 50% at 1350 nm or ΔT = 76.5% at 2500 nm were obtained and are comparable to the state-of-the-art results. The change of the optical constants of VO_2 across the MIT can effectively modulate the infrared transmittance and shift the position of the reflectance valley at 20 °C, leading to a significant enhancement of the IR modulating ability at a certain wavelength.

■ AUTHOR INFORMATION

Corresponding Author

*E-mail: yfgao@mail.sic.ac.cn (Y.G.); hongjieluo@mail.sic.ac.cn (H.L.). Tel/Fax: +86-21-5241-5270.

■ ACKNOWLEDGMENT

This study was supported in part by the Century Program (One-Hundred-Talent Program) of the Chinese Academy of Sciences, National Key Basic Research Project (NKBRP, 2009CB939904), the National Natural Science Foundation of China (NSFC, Contract 50772126), Shanghai Key Basic Research Project (09DJ1400200), Shanghai Basic Research Project (08JC1420300), the key project of the Chinese Academy Sciences (Grant 4912009YC006), and Shanghai Pujiang Talent Program (09PJ1410700).

REFERENCES

(1) Morin, F. J. *Phys. Rev. Lett.* **1959**, *3*, 34–36.

(2) Cao, J.; Ertekin, E.; Srinivasan, V.; Fan, W.; Huang, S.; Zheng, H.; Yim, J. W. L.; Khanal, D. R.; Ogletree, D. F.; Grossmanan, J. C.; Wu, J. *Nat. Nanotechnol.* **2009**, *4*, 732–737.

(3) Stefanovich, G.; Pergament, A.; Stefanovich, D. *J. Phys.: Condens. Matter* **2000**, *12*, 8837–8845.

(4) Cavalleri, A.; Tóh, C.; Siders, C. W.; Squier, J. A.; Ráksi, F.; Forget, P.; Kieffer, J. C. *Phys. Rev. Lett.* **2001**, *87*, 237401.

(5) Kang, L. T.; Gao, Y. F.; Luo, H. J. *ACS Appl. Mater. Interfaces* **2009**, *1*, 2211–2218.

(6) Gurvitch, M.; Luryi, S.; Polyakov, A.; Shabalov, A.; Dudley, M.; Wang, G.; Ge, S.; Yakovlev, V. *J. Appl. Phys.* **2007**, *102*, 033504.

(7) Mlyuka, N. R.; Niklasson, G. A.; Granqvist, C. G. *Phys. Status Solidi A* **2009**, *206*, 2155–2160.

(8) Mlyuka, N. R.; Niklasson, G. A.; Granqvist, C. G. *Appl. Phys. Lett.* **2009**, *95*, 171909.

(9) Burkhardt, W.; Christmann, T.; Franke, S.; Kriegseis, W.; Meister, D.; Meyer, B. K.; Niessner, W.; Schalch, D.; Scharmann, A. *Thin Solid Films* **2002**, *402*, 226–231.

(10) Lee, M.-H.; Cho, J.-S. *Thin Solid Films* **2000**, *365*, 5–6.

(11) Jin, P.; Xu, G.; Tazawa, M.; Yoshimura, K. *Appl. Phys. A: Mater. Sci. Process.* **2003**, *77*, 455–459.

(12) Chen, H. K.; Hung, H. C.; Yang, T. C. K.; Wang, S. F. *J. Non-Cryst. Solids* **2004**, *347*, 138–143.

(13) (a) Li, S.-Y.; Niklasson, G. A.; Granqvist, C. G. *J. Appl. Phys.* **2010**, *108*, 063525. (b) Du, J.; Gao, Y. F.; Luo, H. J.; Zhang, Z. T.; Kang, L. T.; Chen, Z. *Sol. Energy Mater. Sol. Cells* **2011**in press.

(14) Jin, P. Japenese patent 2007171759-A, July 5, 2007.

(15) Lu, C. L.; Cheng, Y. R.; Liu, Y. F.; Liu, F.; Yang, B. *Adv. Mater.* **2006**, *18*, 1188–1192.

(16) Maex, K.; Baklanov, M. R.; Shamiryan, D.; Iacopi, F.; Brongersma, S. H.; Yanovitskaya, Z. S. *J. Appl. Phys.* **2003**, *93*, 8793–8841.

(17) Xu, G.; Jin, P.; Tazawa, M.; Yoshimura, K. *Jpn. J. Appl. Phys.* **2004**, *43*, 186–187.

(18) Kang, L. T.; Gao, Y. F.; Zhang, Z. T.; Du, J.; Cao, C. X.; Chen, Z.; Luo, H. J. *J. Phys. Chem. C* **2010**, *114*, 1901–1911.

(19) Balu, R.; Ashrit, P. V. *Appl. Phys. Lett.* **2008**, *92*, 021904.